ELSEVIER

Biochimica et Biophysica Acta 1321 (1997) 149–156

BIOCHIMICA ET BIOPHYSICA ACTA
BBA

Light-induced electrogenic events associated with proton uptake upon forming Q_B^- in bacterial wild-type and mutant reaction centers

P. Brzezinski [a,1], M.L. Paddock [b], M.Y. Okamura [b], G. Feher [b,*]

[a] *Department of Biochemistry and Biophysics, University of Göteborg and Chalmers University of Technology, Medicinaregatan 9C, S-413 90 Göteborg, Sweden*

[b] *University of California San Diego, Department of Physics 0319, 9500 Gilman Drive, La Jolla, CA 92093-0319, USA*

Received 18 February 1997; revised 12 May 1997; accepted 12 May 1997

Abstract

Light-induced voltage changes (electrogenic events) were measured in wild-type and site-directed mutants of reaction centers (RCs) from *Rhodobacter sphaeroides* oriented in a lipid monolayer adsorbed to a Teflon film. A rapid increase in voltage associated with charge separation was followed by a slower increase attributed to proton transfer from solution to protonatable amino-acid residues in the vicinity of the Q_B site. In native reaction centers the proton-transfer voltage had a pH-dependent amplitude with two peaks at pH 4.5 and pH 9.7, respectively. In the Glu-L212 → Gln RCs the high-pH peak was absent, whereas in the Asp-L213 → Asn RCs the low-pH peak was absent and the high-pH peak was shifted to lower pH by about 1.3 pH units. The amplitudes of the electrogenic phases as a function of pH follow approximately the measured proton uptake from solution (P.H. McPherson, M.Y. Okamura, G. Feher, Biochim. Biophys. Acta, vol. 934, 1988, pp. 348–368) and are ascribed to proton transfer to amino acid residues upon Q_B^- formation. The peak around pH 9.7 is ascribed to proton uptake predominantly by Glu-L212 and the peak around pH 4.5 to proton uptake predominantly by Asp-L213 or a residue strongly interacting with Asp-L213. © 1997 Elsevier Science B.V.

Keywords: Proton transfer; Electron transfer; Bacterial photosynthesis; Electrostatic interaction; (*Rhodobacter sphaeroides*)

1. Introduction

Reaction centers (RCs) from photosynthetic bacteria convert light energy into electrochemical energy. The reaction center is a membrane-spanning protein which contains a number of cofactors involved in this energy-conversion process. In *Rhodobacter sphaeroides* reaction centers this process is initiated by a light-induced excitation of a bacteriochlorophyll dimer (D). An excited electron is then transferred sequentially from D to a pheophytin, to a primary ubiquinone acceptor (Q_A) and a secondary ubiquinone acceptor (Q_B). At each transfer step the electron is

Abbreviations: D, bacteriochlorophyll dimer; Q_A and Q_B, ubiquinones; Q_BH_2, dihydroquinone; CAPS, 3-(cyclohexylamino)propanesulfonic acid; CHES, 2-(cyclohexylaminoethanesulfonic acid); HEPPS, (*N*-2-hydroxyethylpiperazine-*N*′-3-propanesulfonic acid); PIPES, piperazine-*N*,*N*′-*bis*(2-ethanesulfonic acid)

* Corresponding author. Fax: (1) (619) 822-0007; E-mail: gfeher@ucsd.edu

[1] Fax: (+46) (31) 773 3910; E-mail: peter.brzezinski@bcbp.gu.se

PII S0005-2728(97)00052-2

stabilized against charge recombination for progressively longer times. The oxidized donor (D^+) is re-reduced by a water-soluble cytochrome c_2^{2+}. Following a second excitation of D, the secondary quinone becomes doubly reduced and doubly protonated. The dihydroquinone leaves the RC and is replaced by a quinone from a quinone pool in the membrane (for reviews, see [1–3]).

Although in native *Rb. sphaeroides* RCs both Q_A and Q_B are ubiquinones, the energy of the Q_B^- state is lower than that of Q_A^-; the driving force for electron transfer $Q_A^-Q_B \rightarrow Q_AQ_B^-$ is about 60 meV at pH 8.0 [4]. The asymmetry between Q_A and Q_B is due to their different environments. Q_B is surrounded by more negatively charged amino acid residues and water molecules than Q_A [3,5,6,40], resulting in a higher dielectric constant in its vicinity with a concomitant stabilization of the Q_B^- state. An additional contribution has been postulated to be due to the closer proximity of the non-heme Fe^{2+} to Q_B [7].

In the experimentally available pH range the singly reduced quinone Q_B^- is not protonated directly but the interaction of Q_B^- with nearby amino-acid residues increases their pK_a values giving rise to a proton uptake [6,8–12]. These proton-uptake reactions have been studied previously in detergent solutions of RCs using pH electrodes, pH-sensitive dyes, conductance measurements (reviewed in [3]) and infrared spectroscopy [13,14].

In the present study a different approach has been used. Light-induced voltage changes (electrogenic events) associated with proton uptake upon forming Q_B^- were measured in RCs oriented in a phospholipid monolayer adsorbed to a Teflon film [15–19], a technique that was pioneered by Trissl et al. to study rhodopsin [20] and bacteriorhodopsin [21]. This technique makes it possible to monitor the kinetics of electron and proton-transfer reactions in the RC protein.

Upon forming Q_B^- in RCs incorporated in the lipid layer, voltage changes associated with proton-transfer reactions to amino-acid residues in the vicinity of the Q_B site were observed. These voltage changes in native RCs were compared with those measured in mutant RCs in which the protonatable residues Glu-L212 and Asp-L213 were replaced by their non-protonable analogs Gln and Asn, respectively. Preliminary results of this study have been presented [19].

2. Materials and methods

2.1. Materials

Reaction centers from *Rhodobacter sphaeroides* R-26 were purified as described [22] with lauryl dimethylamine *N*-oxide (LDAO, Onyx Chem, NJ) as a solubilizing detergent. Soybean lecithin (type II, Sigma, MO) was purified as described [23]. The construction of the EQ(L212) [Glu-L212 → Gln] and DN(L213) [Asp-L213 → Asn] mutants were described in Paddock et al. [24,25]. Solutions of Terbutryne were prepared in ethanol prior to use.

2.2. Sample preparation

Lipid vesicles containing reaction centers were prepared as described earlier [26]. The phospholipids were dispersed to a final concentration of 10 mg lipid/ml in a buffer composed of 10 mM KCl, 2.5 mM sodium citrate, 2.5 mM PIPES, 2.5 mM HEPPS, 2.5 mM CHES and 2.5 mM CAPS at pH 8.0 (all buffers except sodium citrate were from Calbiochem-Behring) and supplemented with 5 nmole of reaction centers (in ≤ 50 μl) in 0.025% LDAO. The solution was sonicated for 10 minutes at 22 ± 2°C until it was optically clear as determined from the absorbance at 650 nm.

To make RCs with two quinones, phospholipid and ubiquinone (ubiquinone-10, Sigma) were dried together from a hexane solution prior to dispersion in the above described solution. A quinone-to-reaction center ratio of ≥ 100:1 was required to obtain at least 90% of the reaction centers with an active Q_B.

2.3. Monolayer preparation

The experimental set-up is described in detail elsewhere [26,27]. Two aqueous compartments of a Teflon chamber were separated by a 6 μm Teflon sheet (S-25TFE, Saunders Corp., Los Angeles, CA). The side of the Teflon sheet facing the lipid bilayer was treated with 6 μl of 1% (v/v) hexadecane in heptane. The vesicle solution was diluted 1:10 in the buffer described above, supplemented with 10 mM $CaCl_2$ and added to one of the cell compartments to a level just below the Teflon film. After about 5 min. the surface was raised slowly past the Teflon film, allowing the reaction center-lipid monolayer formed at the surface, to adsorb to the Teflon film. The

Teflon-bound reaction center-lipid layer (area 0.3 cm^2) could be illuminated through a window in the chamber. About 60% of the RCs were found to be oriented with the donor facing the aqueous solution [27].

2.4. Electrical measurements

Electrical signals were detected using Calomel (Ingold Electrodes) or Ag/AgCl electrodes, shielded from actinic light. Two different amplifiers were used in this study. One amplifier (Burr-Brown OP128), used for the slower kinetic measurements of charge recombination ($\tau = 0.1$–10 s), had a rise time of ~ 10 μs, an adjustable high input impedance of 10^{10}–10^{11} Ω and a gain of 100. The other amplifier (LF356, National Semiconductors), used for the faster kinetic measurements of the proton-uptake voltage changes, had a rise time of ~ 100 ns, a smaller input impedance of 10^8 Ω and unity gain. It was used as a voltage follower. The signals were then further amplified in a second stage. To improve the signal-to-noise ratio the signals were passed through an RC filter with a variable time constant and averaged using a transient recorder (Nicolet, model 1180 or 490). Pulsed illumination was provided by a dye laser (Phase R, Model DL 1200V) using the dye Rhodamine with a maximum output energy at 590 nm of ~ 100 mJ and a width of ~ 0.4 μs, or a Nd-YAG pulsed laser (Quantel, YG570) at 532 nm with a pulse energy of ~ 20 mJ and a width of ~ 10 ns. Time constants ($1/e$-values) were determined using a non-linear least square procedure on a personal computer.

3. Theory

3.1. Amplitude of the electrogenic signal

The voltage change associated with charge transfer from a donor j to an acceptor k in a lipid layer is assumed to be proportional to the charge transferred and the dielectrically weighted charge-transfer distance [2] along the normal to the monolayer surface [27]. Since the absolute voltage change depends on many factors that vary between preparations, such as the density and orientation of the RCs in the monolayer, we normalized the voltage changes associated with proton transfer to the voltage, (ΔV_{DA}, associated with the charge separation ($DQ_A \rightarrow D^+Q_A^-$), i.e.

$$\frac{\Delta V_{S^cR_i}}{\Delta V_{DA}} = \frac{\epsilon_{DA}}{\vec{d}_{DA}\cdot\vec{n}} \frac{\vec{d}_{S^cR_i}\cdot\vec{n}}{\epsilon_{S^cR_i}} \left(\Delta H^+_{R_i}\right)(\delta) \qquad (1)$$

where $\Delta V_{S^cR_i}$ is the voltage change associated with the transfer of $\Delta H^+_{R_i}$ protons from the cytoplasmic side of the RC (index S^c) to an amino-acid residue R_i; the first and second factors on the right side correspond to the ratio of the dielectrically weighted distances between D and Q_A, and between S^c and R_i (shortest distance) respectively, $\vec{n}$ is a unit vector along the normal to the membrane surface and δ is the fraction of RCs in the $Q_AQ_B^-$ state following a flash. A $\delta < 1$ may be either due to a fraction of reaction centers lacking Q_B and/or due to a fraction of reaction centers in state $Q_A^-Q_B$ after a flash. $\Delta V_{S^cR_i}$, $\Delta H^+_{R_i}$ and δ are pH dependent; distances, dielectric constants and ΔV_{DA} are assumed not to change with pH.

The net proton uptake by R_i interacting electrostatically with Q_B, upon reduction of Q_B is given by [11]:

$$\Delta H^+_{R_i} = \frac{1}{1+10^{pH-pK_{RQ_B^-}}} - \frac{1}{1+10^{pH-pK_{RQ_B}}} \qquad (2)$$

where $pK_{R_iQ_B}$ and $pK_{R_iQ_B^-}$ are the pKs of R_i in the presence of Q_B and Q_B^-, respectively.

By combining Eq. (1) and Eq. (2), and generalizing to n non-interacting amino-acid residues the ratio of the voltage change associated with the proton-uptake, ΔV_{H^+}, to the voltage change associated with the charge separation, ΔV_{DA}, normalized to the fraction, δ, of RCs with Q_B reduced is given by:

$$\begin{aligned}\frac{\Delta V_{H^+}}{\delta\Delta V_{DA}} &= \frac{\epsilon_{DA}}{\vec{d}_{DA}\cdot\vec{n}} \sum_{i=1}^{n} \frac{\vec{d}_{S^cR_i}\cdot\vec{n}}{\epsilon_{S^cR_i}} \\ &\quad\times\left(\frac{1}{1+10^{pH-pK_{RQ_B^-}}} - \frac{1}{1+10^{pH-pK_{RQ_B}}}\right) \\ &= \sum_{i=1}^{n} \varphi_{R_i}\left(\frac{1}{1+10^{pH-pK_{RQ_B^-}}}\right. \\ &\quad\left. - \frac{1}{1+10^{pH-pK_{RQ_B}}}\right) \qquad (3)\end{aligned}$$

[2] The dielectrically weighted distance is defined as the distance divided by an effective dielectric constant, ϵ, of the medium spanning the charge transfer path.

where φ_{R_i} is the ratio of the dielectrically weighted distances. It is equal to the ratio of the voltage associated with the transfer of *one* proton to R_i to the charge separation voltage, V_{DA}.

Each term of the sum in Eq. (3) represents a peak with its maximum value at $pH = (pK_{R_iQ_B^-} + pK_{R_iQ_B})/2$. The largest value of this maximum (= 1) occurs when $(pK_{R_iQ_B^-} - pK_{R_iQ_B}) > 3$. For every residue the shape of this peak is described by three parameters φ_{R_i}, $pK_{R_iQ_B}$ and $pK_{R_iQ_B^-}$.

In the above treatment, we have neglected interaction between amino acid residues. This is a serious over-simplification as these interactions may be quite large and significant [6,9–12,24,25,28–36]. Nevertheless, they serve to characterize the different RCs and create a framework in which to discuss experimentally observed differences.

4. Results

Reaction centers (RCs) were oriented in lipid monolayers adsorbed to a Teflon film. Following pulsed illumination of the RC-lipid layer an increase in voltage, associated with charge separation was followed by a slower decrease associated with charge recombination (Fig. 1). The voltage change due to charge recombination was decomposed into two components with time constants of about 100 ms and about 1 s associated with charge recombination of $D^+Q_A^-$ and $D^+Q_AQ_B^-$, respectively [4]. The fraction of electrons on Q_B following charge separation was determined from the fraction of the slow component in the recombination voltage change. This fraction was large as can be seen in the example shown in Fig. 1.

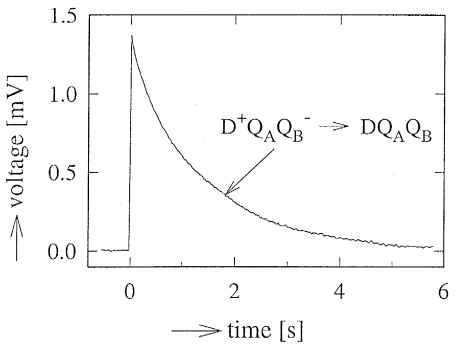

Fig. 1. Voltage changes from reaction centers incorporated in a lipid monolayer absorbed to a teflon sheet following illumination. The measured relaxation time (~ 1s) corresponds to the characteristic $D^+Q_AQ_B^- \rightarrow DQ_AQ_B$ recombination time for RCs in solution. Conditions: 2.5 mM sodium citrate, 2.5 mM PIPES, 2.5 mM HEPPS, 2.5 mM CHES and 2.5 mM CAPS at pH 8.0, 10 mM KCl, 10 mM CaCl2, 0.5 μM reaction centers, 1 mg/ml lipids, ~ 50 UQ_{10}/reaction center, $T = 20 \pm 1$°C.

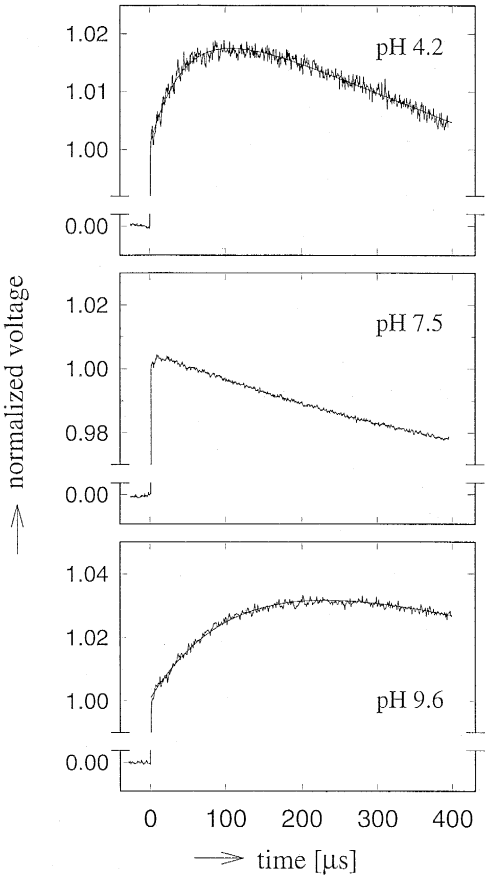

Fig. 2. Voltage changes following pulsed illumination of native RCs incorporated in a lipid monolayer at different pHs. Note the different time scale from that used in Fig. 1. Voltage changes were normalized to the charge-separation voltages and fraction of Q_B reduced. A voltage decay with a time constant of ~ 200 μs previously reported to follow charge separation both in one- and two-quinone reaction centers [17] has been subtracted from the traces. The decay that was subtracted was measured in RCs after addition of 50 μM terbutryne to inhibit Q_B activity. The noise-free lines are least-square fits of a sum of two exponentials to the data — the faster one represents the voltage change associated with proton uptake (see Section 5), the slower one is the time constant of the amplifier used for these measurements. The amplitudes of the faster component associated with proton uptake are shown versus pH in Fig. 3. Conditions were the same as in Fig. 1, except the pH was varied as indicated.

In Fig. 2 the light-induced voltage changes at three different pH values are shown on a shorter time scale. A voltage decay with a time constant of about 200 μs [17], measured in one-quinone reaction centers was subtracted from the data. A rapid (<100 ns) increase in voltage was followed by a slower increase with a time constant of ~ 100 μs below pH 7, consistent with a net positive charge moving into the reaction centers from the cytoplasmic side, e.g. proton uptake upon forming Q_B^- (see Section 5).

The voltage changes shown in Fig. 2 were normalized to the charge separation voltage changes and the fraction of the slow charge recombination component, i.e. to the fraction, δ of Q_B^- formed following pulsed illumination (cf. Eq. (3)). The latter correction was based on the assumption that only those reaction centers that display a slow recombination contribute to proton uptake following charge separation. This correction was negligible below pH $\cong$ 9 (i.e. $\delta \cong 1$).

Fig. 3 shows the amplitudes of the voltage changes as a function of pH between pH 4 and 11. Two peaks are observed; one around pH 9.7 with a maximum value of $\sim$ 5% of the charge-separation voltage and one around pH 4.5 with a maximum value of $\sim$ 2.5% of the charge-separation voltage. These results are consistent with those observed in isolated chromatophores [37]. Fig. 4 shows the voltage changes as a function of pH in two mutant RCs in which protonatable amino-acid residues close to the Q_B binding site (Fig. 5) have been replaced with their non-protonata-

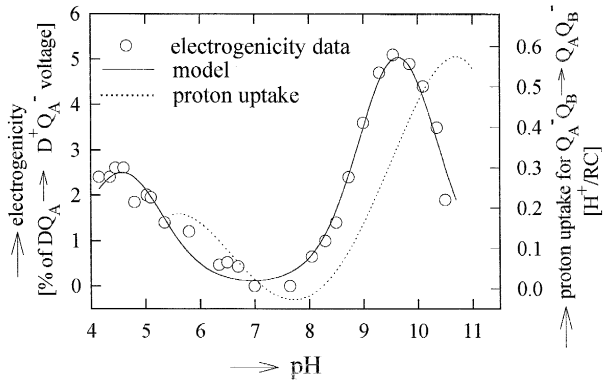

Fig. 3. Voltage changes upon forming Q_B^- associated with proton uptake as a function of pH in native reaction centers (circles). The amplitudes were determined from the least-square fits of the kinetic data (see legend of Fig. 2). The solid line is a fit to Eq. (3) using parameters shown in Table 1. Also shown is the measured proton uptake from RCs in solution for the reaction $Q_A^-Q_B \rightarrow Q_AQ_B^-$ determined with pH sensitive dyes (dotted line is the differential proton uptake, $\Delta H^+(Q_AQ_B^-) - \Delta H^+(Q_A^-Q_B)$, corresponding to the electron transfer; taken from figures 5 and 6 of [11]). The qualitative agreement between the electrogenic signals and proton uptake show that surface residues (which do not contribute to the electrogenic voltage signals) play at most a minor part in proton uptake associated with the electron transfer $Q_A^-Q_B \rightarrow Q_AQ_B^-$.

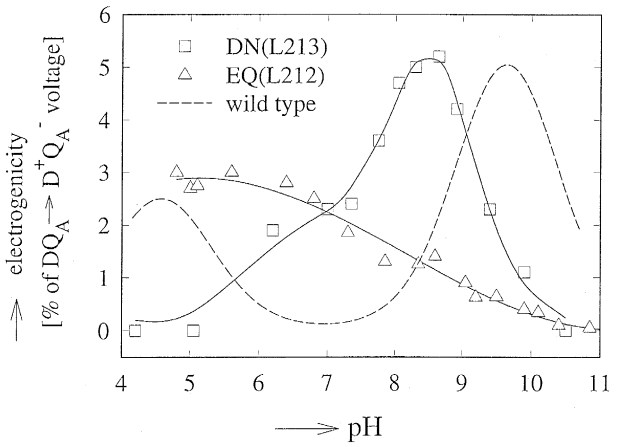

Fig. 4. Voltage changes upon forming Q_B^- as a function of pH in EQ(L212) (triangles, $\triangle$) and DN(L213) (squares, $\square$) mutant RCs. The dashed line corresponds to native RCs (see Fig. 3). In the EQ(L212) mutant RCs the high pH peak and in the DN(L213) mutant RCs the low pH peak are absent. These results were used to identify the peak with the titration of Glu-L212 and Asp-L213, respectively.

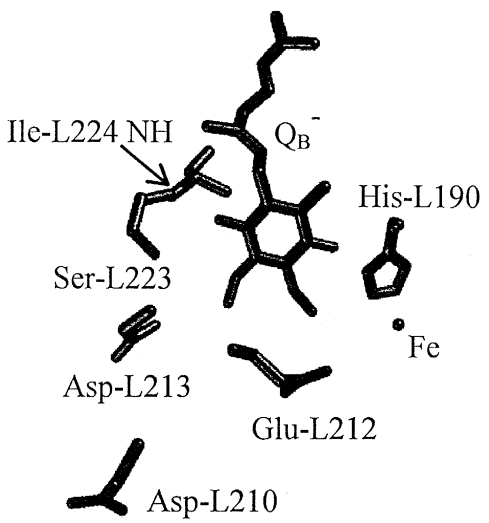

Fig. 5. The position of the protonatable residues Glu-L212, Asp-L213, Asp-L210, and His-L190 in relation to Q_B^-. The lower part of this figure corresponds to the cytoplasmic side of the RC (coordinates from [40]).

ble analogs. These are Glu-L212 → Gln [EQ(L212)] and Asp-L213 → Asn [DN(L213)] [24,25,30,31]. In the EQ(L212) mutant RCs the high-pH peak was absent. In the DN(L213) mutant RCs the high-pH peak was shifted by ~1.3 pH units to lower pH and the low-pH peak was absent.,,,

5. Discussion

Voltage changes in reaction centers oriented in lipid monolayers were measured following pulsed illumination. A rapid increase in voltage associated with charge separation was followed by a slower increase with a time constant of ~100 μs below pH 7. The time constant of this voltage change was similar to that of the electron transfer $Q_A^- Q_B \rightarrow Q_A Q_B^-$. This voltage change was associated with reduction of Q_B and not with oxidation of D because it was observed also in the presence of reduced cytochrome c_2 which re-reduced D^+ on a shorter time scale than 100 μs. We have previously reported voltage changes associated with Q_A^- formation on the same time scale but of opposite sign [17]. This voltage change was subtracted from the traces shown in Fig. 2 (see figure legend).

The results show that charges redistribute within the reaction centers upon formation of Q_B^-. This charge redistribution could in principle be associated with electron transfer, proton transfer or structural changes. We attribute the increase in voltage following reduction of Q_B to proton uptake using the following arguments: (1) The pH dependence of the amplitude of the electrogenic phase agrees favorably with the proton uptake measured in solution for $Q_A^- Q_B \rightarrow Q_A Q_B^-$ [11] (see Fig. 3) [3]. (2) The pH dependence of the voltage change in the EQ(L212) and DN(L213) mutant RCs was consistent with the proton-uptake and charge recombination characteristics of these mutant RCs [24,25,31]. (3) The rate of the voltage change displayed a pH dependence consistent with proton uptake (not shown). It was not consistent with a possible small electrogenicity associated with electron transfer $Q_A^- Q_B \rightarrow Q_A Q_B^-$, whose rate is essentially independent of pH in the range of 4 to 9 and above pH ~9 drops by a factor of ~ten per pH unit with a pK of 9.8 [4]. (4) The sign of the voltage changes is consistent with a positive charge moving into the RCs from the cytoplasmic side of the RC [4].

The measured voltage changes shown in Fig. 3 were fitted with the mathematical expression of Eq. (3) using a least-square procedure. A good fit was obtained using two protonatable groups with their pK_a values in the presence of Q_B and Q_B^- as adjustable parameters (Table 1). Since the low-pH peak could be fitted with any $pK_{R_i Q_B} \leq 4$, it was not possible to determine from the data whether this peak was due to protonation of an amino-acid residue with a $pK_{R_i Q_B} \leq 4$ or a direct protonation of Q_B^-. However, direct optical measurements have shown that the semiquinone is not protonated down to pH 4 [39], therefore, it is unlikely that the low-pH peak in Fig. 3 is due to direct protonation of Q_B^-.

Table 1
Parameters used to fit the data in Fig. 3 to Eq. (3)

	pK_a of R_i when Q_B is uncharged	pK_a of R_i when Q_B is charged (Q_B^-)	φ_{R_i} [a]
$i=1$	3.9 [b]	5.1±0.3	4.3±0.5
$i=2$	9.1±0.1	10.2±0.1	11±3

[a] φ_{R_i} is the ratio of the dielectrically weighted distance from the RC surface to R_i to the distance D to Q_A (see Eq. (3)).
[b] Since measurements below pH 4 were not possible, this represents an upper limit for the pK_a value of the low pH titrating group.

[3] One can make a rough calibration of the electrogenic phase to a proton uptake amplitude using the magnitude of the electrogenic signal after the second flash (~12–17% of the charge separation voltage [37,38]), as a normalization factor for 2 H^+/RC (i.e. 1 H^+/RC corresponds to 6–8.5% of the charge separation voltage). This inherently assumes that the dielectrically weighted distance is the same for all protons whether they traverse the protein to the quinone or to a buried amino acid residue. Although this assumption is rather rough, we shall use it to make a qualitative estimate of proton uptake. The high pH peak would correspond to ~0.6–0.9H^+/RC and the low pH peak to ~0.3–0.4H^+/RC. Given the implicit assumptions, these estimates compare favorably with the measured proton uptake of 0.6H^+/RC and 0.15H^+/RC for the high and low pH peaks using pH-sensitive dyes [11], respectively.

[4] In principle, the signal could be due to any positive charge (ion) moving into the RC interior. However, ions in solution should not show an electrogenic signal, since their contribution to the Q_A^- signal are expected to be approximately the same as to the Q_B^- signal.

To identify the amino-acid residues involved in proton uptake, voltage changes were measured in two types of mutant reaction centers in which protonatable amino-acid residues close to the Q_B binding site (Fig. 5, [40]) were replaced by their non-protonatable analogs [19]. The replacement of Glu-L212 with Gln resulted in the disappearance of the peak around pH 9.7. Consequently, the high-pH peak in the wild-type reaction centers was ascribed to proton uptake predominantly by Glu-L212 [5]. This is consistent with the pH-dependences of the $D^+Q_B^- \rightarrow DQ_B$ recombination times in native and EQ(L212) mutant RCs [24], which shows that Glu-L212 has an apparent pK_a of pH 9.5 with Q_B oxidized, which shifts to higher pH upon formation of Q_B^-. In addition, measurements of proton uptake from solution upon forming the state $DQ_AQ_B^-$ in native and EQ(L212) mutant RCs have shown that Glu-L212 has a significant contribution to proton uptake at pH 9.5 [41,42]. Assuming classic titration for Glu-L212, these results are seemingly in conflict with time-resolved infrared measurements which show that Glu-L212 is partially (30–50%) ionized at pH 8 [13,14]. This apparent discrepancy can be explained by non-classic titration of Glu-L212 due to strong interactions with other titrating residues [6,12–14,28,29,43]. The larger electrogenic signal around pH 7 observed in the EQ(L212) RCs suggests that some other titrating site now contributes to the observed electrogenic phases in the absence of Glu-L212. This signal can represent compensating proton uptake by some other titrating acid(s) in the vicinity of Q_B. This supports the suggestion of large electrostatic interactions inside the protein [6,9–12,24,25,28,29].

The replacement of the protonatable residue Asp-L213 with its non-protonatable analog Asn resulted in the disappearance of the peak around pH 4.5 and a shift of the high-pH peak by 1.3 units to lower pH. The shift of the high-pH peak in the Asp-L213 mutant RCs can be interpreted in terms of electrostatic interactions between the ionized Asp-L213 and Glu-L212. If the pK of Asp-L213 is low (<7) it carries a negative charge in the pH region where Glu-L212 titrates. When this charge is replaced by a neutral species, as in the DN(L213) mutant RCs, the pK of Glu-L212 shifts to lower pH.

The absence of the low-pH peak in the DN(L213) mutant RCs suggests that this peak in the native RCs is associated with either (i) protonation of Asp-L213 itself or (ii) protonation of another residue, e.g. Asp-L210 [44], whose pK is strongly influenced by the ionization state of Asp-L213 (Fig. 5). Upon mutation of Asp-L213, the pK of the titrating residue would be moved outside the experimentally available pH range. The observation that the amplitude of the lower pH peak is smaller than the high pH peak indicates a larger distance between the titrating site and Q_B^-, more consistent with the identity of the titrating site being Asp-L210 [44], located further from Q_B than Glu-L212.

While proton-uptake measurements using pH meters or pH-sensitive dyes involve *all* protons taken up by the reaction centers, including those of surface groups, electrogenicity measurements are expected to be only sensitive to those proton-transfer reactions that take place within the reaction centers and have a component perpendicular to the membrane surface. The qualitative agreement of the pH dependence of the electrogenicity upon Q_B^- formation with the proton-uptake from solution associated with electron transfer $Q_A^-Q_B \rightarrow Q_AQ_B^-$ (Fig. 3) shows that residues buried inside the RC are primarily involved in proton uptake. The differences between the two sets of data shown can be attributed to either pK_a shifts of the amino acid residues due to differences in the sample conditions (e.g. detergent compared to lipid monolayer, salt concentration) or to contribution of surface groups to the proton uptake data. In conclusion, electrogenic measurements, such as those presented in this work, provide complementary data to proton uptake measurements performed with other techniques and can help distinguish internal reactions from surface reactions.

[5] The notion that an observed proton uptake peak can be attributed to a single titrating acid is an approximation. If electrostatic interactions between many acids are present, all coupled titrating acids contribute to the observed proton uptake (see the simple example of two coupled acids presented in the appendix of Ref. [25]). However, the magnitude of the individual contributions vary depending upon the intrinsic pK_a's and interaction energies. In the present model the contribution of Glu-L212 predominates at pH 9.7 due to its higher intrinsic pK_a. The FTIR [14] and kinetic IR [13] signals observed at lower pH at 1728 cm^{-1} are attributed to Glu-L212 which has a broader non-classic titration curve due to interactions with other internal titrating acids.

Acknowledgements

We thank R. Isaacson for technical assistance and E. Abresch for the preparation of reaction centers. This study has been supported by grants from NSF (MCB94-16652), NIH (GM 13191) and the Swedish Natural Science Research Council.

References

[1] G. Feher, J.P. Allen, M.Y. Okamura, D.C. Rees, Nature 339 (1989) 111–116.
[2] M. Gunner, Current Topics in Bioenergetics 16 (1991) 319–367.
[3] M.Y. Okamura, G. Feher, Annu. Rev. Biochem. 61 (1992) 861–896.
[4] D. Kleinfeld, M.Y. Okamura, G. Feher, Biochim. Biophys. Acta 766 (1984) 126–140.
[5] P. Beroza, D.R. Fredkin, M.Y. Okamura, G. Feher, in: J. Breton and A. Verméglio (Eds.), The Photosynthetic Bacterial Reaction Center II, Plenum Press, New York, 1992, pp. 363–374.
[6] U. Ermler, G. Fritzsch, S.K. Buchanan, H. Michel, Structure 2 (1994) 925–936.
[7] J.P. Allen, G. Feher, T.O. Yeates, H. Komiya, D.C. Rees, Proc. Natl. Acad. Sci. USA 85 (1988) 8487–8491.
[8] C.A. Wraight, Biochim. Biophys. Acta 548 (1979) 309–327.
[9] P. Maróti, C.A. Wraight, Biochim. Biophys. Acta 934 (1988) 314–328.
[10] P. Maróti, C.A. Wraight, Biochim. Biophys. Acta 934 (1988) 329–347.
[11] P.H. McPherson, M.Y. Okamura, G. Feher, Biochim. Biophys. Acta 934 (1988) 348–368.
[12] M.R. Gunner, B. Honig, in: J. Breton, A. Verméglio (Eds.), The Photosynthetic Bacterial Reaction Center II: Structure, Spectroscopy and Dynamics, Plenum Press, New York/London, 1992, pp. 403–410.
[13] R. Hienerwadel, S. Grzybek, C. Fogel, W. Kreutz, M.Y. Okamura, M.L. Paddock, J. Breton, E. Nabedryk, W. Mäntele, Biochemistry 34 (1995) 2832–2843.
[14] E. Nabedryk, J. Breton, R. Hienerwadel, C. Fogel, W. Mäntele, M.L. Paddock, M.Y. Okamura, Biochemistry 34 (1995) 14722–14732.
[15] Y. Blatt, A. Gopher, M. Montal, G. Feher, Biophys. J. (abstr.) 41 (1983) 121a.
[16] G. Feher, M.Y. Okamura, in: C. Sybesma (Ed.), Advances in Photosynthesis Research, Vol. II, Martinus Nijhoff/Dr W. Junk Publishers, The Hague, 1984, pp. 155–164.
[17] P. Brzezinski, M.Y. Okamura, G. Feher, in: J. Breton and A. Verméglio (Eds.), The Photosynthetic Bacterial Reaction Center II: Structure, Spectroscopy and Dynamics, Plenum Press, New York, 1992, pp. 321–330.
[18] F. Höök, P. Brzezinski, Biophys. J. 66 (1994) 2066–2072.
[19] P. Brzezinski, M.L. Paddock, S.H. Rongey, M.Y. Okamura, G. Feher, Biophys. J. (abstr.) 59 (1991) 143a.
[20] H.-W. Trissl, A. Darszon, M. Montal, Proc. Natl. Acad. Sci. USA 74 (1977) 201–210.
[21] H.-W. Trissl, M. Montal, Nature 266 (1977) 655–657.
[22] G. Feher, M.Y. Okamura, in: R.K. Clayton, W.R. Sistrom (Eds.), The Photosynthetic Bacteria, Plenum Press, New York, 1978, pp. 349–386.
[23] Y. Kagawa, E. Racker, J. Biol. Chem. 246 (1971) 5477–5487.
[24] M.L. Paddock, S.H. Rongey, G. Feher, M.Y. Okamura, Proc. Natl. Acad. Sci. USA 86 (1989) 6602–6606.
[25] M.L. Paddock, S.H. Rongey, P.H. McPherson, A. Juth, G. Feher, M.Y. Okamura, Biochemistry 33 (1994) 734–745.
[26] A. Gopher, Y. Blatt, M. Schönfeld, M.Y. Okamura, G. Feher, M. Montal, Biophys. J. 48 (1985) 311–320.
[27] P. Brzezinski, A. Messinger, Y. Blatt, A. Gopher, D. Kleinfeld (submitted to Membrane Biology).
[28] P. Beroza, D.R. Fredkin, M.Y. Okamura, G. Feher, Biophys. J. 68 (1995) 2233–2250.
[29] C.R.D. Lancaster, H. Michel, B. Honig, M.R. Gunner, Biophys. J. 70 (1996) 2469–2492.
[30] E. Takahashi, C.A. Wraight, Biochim. Biophys. Acta 1020 (1990) 107–111.
[31] E. Takahashi, C.A. Wraight, Biochem. 31 (1992) 855–866.
[32] E. Takahashi, C.A. Wraight, in: J. Barber (Ed.), Advances in Molecular and Cell Biology, JAI Press, Greenwich, CT, 1994, pp. 197–251.
[33] E. Takahashi, C.A. Wraight, in: P. Mathis (Ed.), Photosynthesis: From Light to Biosphere, Kluwer Academic Publishers, Dordrecht, 1995, pp. 691–694.
[34] E. Takahashi, C.A. Wraight, Proc. Natl. Acad. Sci. USA 93 (1996) 2640–2645.
[35] P. Sebban, P. Maroti, M. Schiffer, D.K. Hanson, Biochemistry 34 (1995) 8390–8397.
[36] P. Sebban, P. Maroti, D.K. Hanson, Biochimie 77 (1995) 677–694.
[37] L.A. Drachev, M.D. Mamedov, A.Ya. Mulkidjanian, A.Yu. Semenov, V.P. Shinkarev, M.I. Verkhovsky, FEBS Letters 259 (1990) 324–326.
[38] P. Brzezinski, M.L. Paddock, M.Y. Okamura, G. Feher, Biophys. J. (abstr.) 59 (1991) 143a.
[39] M.S. Graige, M.L. Paddock, J.M. Bruce, G. Feher, M.Y. Okamura, J. Am. Chem. Soc. 118 (1996) 9005–9016.
[40] M.H.B. Stowell, T.M. McPhillips, D.C. Rees, S.M. Soltis, E. Abresch, G. Feher, Science 276 (1997) 812–816.
[41] P.H. McPherson, M. Schönfeld, M.L. Paddock, M.Y. Okamura, G. Feher, Biochemistry 33 (1994) 1181–1193.
[42] J. Miksovska, P. Maroti, J. Tandori, M. Schiffer, D.K. Hanson, P. Sebban, Biochemistry 35 (1996) 15411–15417.
[43] P. Beroza, D.R. Fredkin, M.Y. Okamura, G. Feher, Proc. Natl. Acad. Sci. USA 88 (1991) 5804–5808.
[44] M.L. Paddock, A. Juth, G. Feher, M.Y. Okamura, Biophys. J. (abstr.) 61 (1992) A153.